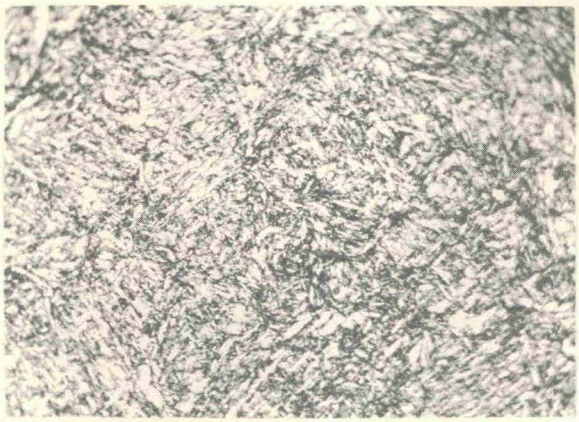

(a)

(b)

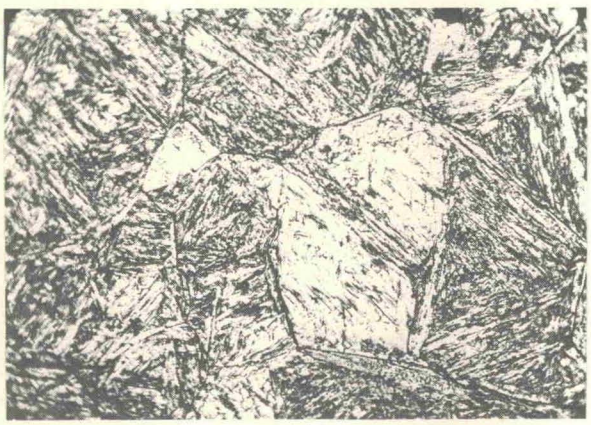

(c)

FIG. 4. (a) Typical Fe-Mn unshocked microstructure following a water quench. Magnification is 500×. Austenitic grain boundaries are hidden. (b) Shock-loaded Fe-7Mn at 300 kbar, showing mixed microstructure. Austenitic grain boundaries have reappared due to the retainment of the high-pressure fcc phase. Magnification is 500×. (c) Microstructure of the shocked Fe-7Mn. Typical martensitic structure is shown, with prior austenitic grain boundaries. Magnification is 500×.

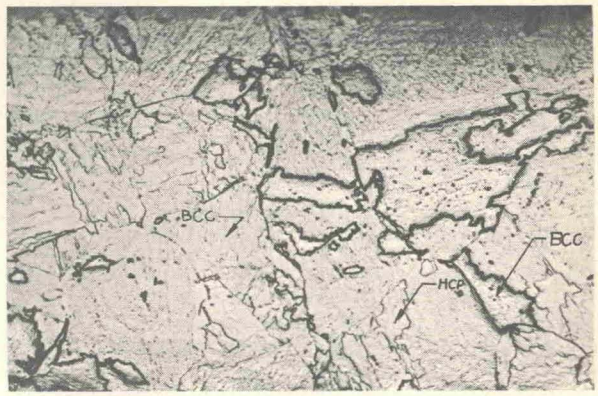

(a)

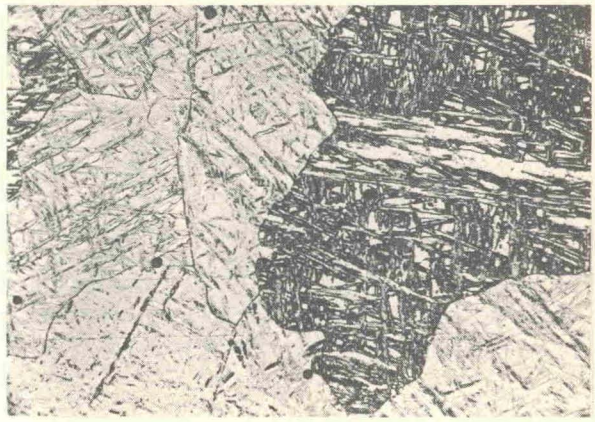

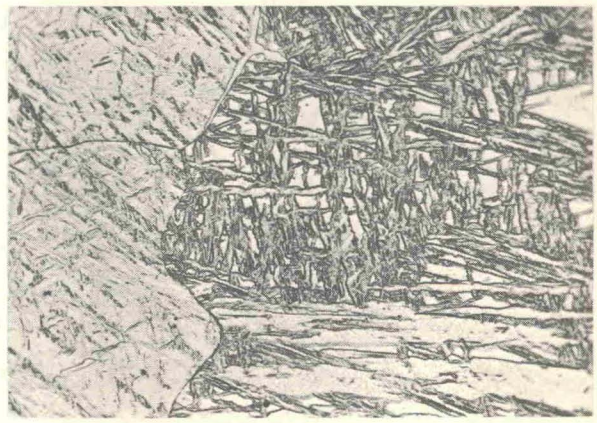

(b)

FIG. 5. (a) Microstructure of Fe-7Mn slow cooled from 900 °C. The hcp phase is outlined by the lightly etched grain boundaries. The matrix is bcc. These observations have been verified by the electron probe. Magnification is 250×. (b) Microstructure of Fe-7Mn, slow cooled and shock loaded to 300 kbar. Profuse twinning is evident. Magnification is 500×.

specimens clearly indicate that the high-pressure phase has been retained in the alloys Fe-4Mn to Fe-14Mn, which were shock loaded at pressures above 90 kbar. The maximum density change occurred after shock deformation at 300 kbar for Fe, Fe-0.4Mn, and Fe-4Mn and at 500 kbar for Fe-7Mn and Fe-14Mn. From 300–500 kbar there was no appreciable change in the retention of the close-packed phases. No appreciable density changes were observed in the Fe and Fe-0.4Mn alloys. The density change was much less in the alloys which were initially furnace cooled prior to shock deformation. The residual density changes are believed to be due to an $\alpha' \rightarrow \gamma$ or $\alpha' \rightarrow \epsilon$ transformation. The stability of the shock-

TABLE II. Density changes in shock deformed Fe-Mn alloys.

Alloy	Heat treatment	Initial density ρ_0 (g/cm^3) at 20 °C	Density changes[a] 90 kbar	150 kbar	300 kbar	500 kbar
Fe	900 °C, water quench	7.8711	1.0001	1.0002	1.0002	1.0002
Fe-0.4Mn	900 °C, water quench	7.8716	1.0002	1.0002	1.0003	1.0003
Fe-4Mn	950 °C, water quench	7.8698	1.0023	1.0097	1.0146	1.0140
Fe-7Mn	950 °C, water quench	7.9088	1.0028	1.0028	1.0218	1.0431
Fe-14Mn	950 °C, water quench	7.9902	1.0275	1.0392	1.0449	1.0450
Fe	900 °C, furnace cool	7.8712	1.0001	1.0002	1.0002	1.0002
Fe-0.4Mn	900 °C, furnace cool	7.8719	1.0002	1.0002	1.0002	1.0003
Fe-4Mn	950 °C, furnace cool	7.8722	1.0002	1.0006	1.0007	1.0007
Fe-7Mn	950 °C, furnace cool	7.9135	1.0003	1.0006	1.0007	1.0008
Fe-14Mn	950 °C, furnace cool	7.9939	1.0008	1.0008	1.0009	1.0009

[a]Density change = density after shock loading (ρ_s)/unshocked density (ρ_0).

produced close-packed phases was exhibited by quenching them to 78 °K and causing only a slight change in the density ratio (less than 0.15%). It is emphasized that the retained close-packed phase which was produced by shock primarily came from the bcc martensite with manganese content in the range of 4-16 wt%. The retained high-pressure phase increased with the manganese content of the bcc phase. The slow-cooled alloys contained bcc martensite with 2—4 wt% Mn, and, consequently, the retainment of the high-pressure phase was not possible.

B. Structure Determination

X-ray diffraction data of all alloys were taken before and after shocking at 90, 150, and 300 kbar. The x-ray diffraction results indicate that, for the Fe-4Mn and Fe-7Mn alloys, the γ phase has been stabilized at room temperature after shock deformation, while the ϵ phase has been stabilized for the Fe-14Mn alloy. The unshocked quenched Fe, Fe-0.4Mn, and Fe-4Mn specimens produced the diffraction lines of bcc Fe-Mn; equilibrium bcc and martensitic bcc lines were not separable. The α' lattice parameter was found to increase linearly with increasing solute content up to 14 wt% Mn. The unshocked quenched Fe-7Mn and Fe-14Mn specimens produced the diffraction lines of bcc martensite. The quenched and shocked Fe and Fe-0.4Mn specimens showed the same lines as the unshocked specimens. However,

TABLE III. X-ray diffraction data of Fe-Mn shock loaded up to 300 kbar.

P (kbar)	d(bcc) (Å)	$(hkl)_{bcc}$	a(bcc) (Å)	d(hcp) (Å)	$(hkl)_{hcp}$	a(hcp) (Å)	c(hcp) (Å)	d(fcc) (Å)	$(hkl)_{fcc}$	a(fcc) (Å)
Fe-14Mn										
unshocked	2.05±0.05	(110)	2.85							
	1.40±0.05	(200)								
	1.20±0.03	(211)								
150	~2.04±0.05	(110)	2.83	1.90±0.05	(101)	2.45	3.95			
	1.40±0.08	(200)		~2.00±0.06	(002)					
	~1.19±0.05	(211)								
300	~2.04±0.05	(110)	2.83	2.14±0.06	(100)	2.45	3.95			
	1.40±0.05	(200)		~2.00±0.08	(002)					
	1.17±0.07	(211)		~1.90±0.08	(101)					
				1.45±0.05	(102)					
				1.25±0.07	(110)					
				1.15±0.07	(103)					
Fe-7Mn										
unshocked	~2.00±0.02	(110)	2.80							
	1.38±0.02	(200)								
	1.21±0.03	(211)								
300	~2.00±0.05	(110)	2.80					2.06±0.05	(111)	~3.50
[Fe-7Mn]	1.40±0.06	(200)						1.80±0.05	(200)	~3.50
	1.20±0.05	(211)						1.30±0.05	(220)	~3.47
Fe-4Mn										
unshocked	~1.98±0.05	(110)	2.79							
	1.38±0.02	(200)								
	1.20±0.03	(211)								
300								2.05±0.05	(111)	~3.50
								1.79±0.05	(200)	~3.49
								1.32±0.05	(220)	~3.48